Optical-field–induced refractive indices and orientational relaxation times in a homologous series of isotropic nematic substances*

E. G. Hanson and Y. R. Shen†

Department of Physics, University of California, and Materials and Molecular Research Division, Lawrence Berkeley Laboratory, Berkeley, California 94720

G. K. L. Wong

Physics Department, Northwestern University, Evanston, Illinois 60201

(Received 15 March 1976)

We have measured the optical Kerr constant and the orientational relaxation times of seven p,p'-di-n-alkoxyazoxybenzene homologous compounds as functions of temperature in the isotropic phase. The observed critical behaviors near the isotropic-nematic transitions agree well with the predictions from the Landau–de Gennes model. Various characteristic parameters of the homologs are deduced from the experiment. Their variations with increase of methylene groups in the alkyl chain are discussed. Our results suggest that neither the mean-field theory of Maier and Saupe nor the Landau expansion of free energy is a good approximation for quantitative description at the isotropic-nematic transition.

I. INTRODUCTION

Recently, it has been demonstrated by nonlinear optical measurements that liquid-crystalline materials in their isotropic phase can have a large optical Kerr constant with a long relaxation time.[1] Such characteristics result from the pretransitional behavior of the materials. The nonlinear optical measurements actually provide a stringent test of the Landau–de Gennes phase-transition model for liquid crystals. From these measurements, together with measurements of the order parameter and anisotropy in refractive indices, one can obtain values for a large number of characteristic material parameters: T^*, the fictitous second-order isotropic-nematic transition temperature; ν, the viscosity coefficient for molecular orientation; a, b, and d, the coefficients in the Landau-series expansion of the free energy, etc. These parameters are important for characterizing a liquid-crystalline material. To understand how molecular structure affects the properties of liquid crystals, it will be of great interest to find these parameters for a homologous series of compounds. However, no such information for any homologous series exists in the literature.

In this paper, we report the results of our recent nonlinear refractive-index measurements on the homologous compounds of p,p'-di-n-alkoxyazoxybenzenes. The molecular structures of these compounds are shown in Table I. Also listed in Table I are the isotropic nematic-transition temperatures T_K of our samples, the macroscopic order parameters Q_K at T_K, optical susceptibility anisotropies $\Delta\chi$ (defined for the case of perfect molecular alignment) we measured recently, and the latent heats ΔH obtained from Ref. 2. From the nonlinear optical measurements and the values of T_K, Q_K, and $\Delta\chi$, we deduce the various characteristic parameters we mentioned earlier for these homologous compounds. The work here constitutes one of the very few examples where nonlinear optical measurements can yield quantitative results not only on nonlinear optical coefficients but also on other characteristic parameters of a condensed matter.

In Sec. II, we give a brief review of the theory of optical-field–induced refractive indices. We describe in Sec. III the experimental arrangement and the data-analysis procedure. Then in Sec. IV we present the experimental results and the material parameters deduced from our results. Finally, Sec. V discusses the implications of our results from the molecular structural viewpoint.

II. THEORETICAL BACKGROUND

Liquid-crystalline materials are composed of highly anisotropic molecules. Consequently, the induced dipoles on the molecules are also highly anisotropic. In the presence of intense optical field, the molecules tend to be aligned by the field via induced-dipole interaction with the field. The resultant molecular ordering is then reflected by the induced optical anisotropy in the medium.

If Q is a macroscopic tensorial order parameter which describes the degree of molecular alignment, then the optical susceptibility χ_{ij} (or any tensorial property of the medium) can be written[3]

$$\chi_{ij} = \bar{\chi}\delta_{ij} + \tfrac{2}{3}\Delta\chi Q_{ij}\,, \tag{1}$$

TABLE I. Molecular structures and other characteristic parameters of the p,p'-di-n-alkoxy-azoxybenzene homologs.

Structure: $CH_3-(CH_2)_{N-1}-O-(C_6H_4)-N_2O-(C_6H_4)-O-(CH_2)_{N-1}-(CH_3)$				
N	T_K (°C)	Q_K	$10^{+3}\Delta\chi$	ΔH_{expt} (10^6 erg/cm^3)
1	132.7	0.400	108.9	25.4
2	163.1	0.517	97.1	52.5
3	119.95	0.395	87.2	22.8
4	129.9	0.475	79.0	31.4
5	118.6	0.358	74.9	19.9
6	123.9	0.437	64.5	26.2
7	119.3	0.431	60.9	23.5

where $\bar{\chi}=\frac{1}{3}\Sigma_i\chi_i$ and $\Delta\chi$ is the anisotropy in χ_{ij} with perfect molecular alignment such that $\frac{1}{2}Q_{xx}=-Q_{yy}=-Q_{zz}=\frac{1}{2}$. In the absence of field, in an isotropic medium Q_{ij} is zero, but becomes finite in the presence of a field. According to the Landau–de Gennes model,[3] the free energy per unit volume of an isotropic fluid in the presence of an intense field $\vec{E}(\omega)$ and a weak probing field $\vec{E}(\omega')$ is given by

$$F=F_0+\tfrac{1}{2}a(T-T^*)Q_{ij}Q_{ji}+\tfrac{1}{3}bQ_{ij}Q_{jk}Q_{ki}+\tfrac{1}{4}dQ_{ij}Q_{jk}Q_{kl}Q_{li}-\tfrac{1}{4}\chi_{ij}(\omega)E_i^*(\omega)E_j(\omega)-\tfrac{1}{4}\chi_{ij}(\omega')E_i^*(\omega')E_j(\omega'), \quad (2)$$

where F_0 is independent of Q. The field-induced molecular ordering then obeys the dynamic equation[3] $\nu\partial Q_{ij}/\partial t=-\partial F/\partial Q_{ji}$. Normally, Q is small in the isotropic phase, and hence the Q^3 and Q^4 terms and the $\chi_{ij}(\omega')E_i^*(\omega')E_j(\omega')$ term in Eq. (2) are often negligible. The dynamic equation assumes the form

$$\nu\frac{\partial Q_{ij}}{\partial t}+a(T-T^*)Q_{ij}=f_{ij}(t),\qquad f_{ij}=\tfrac{1}{12}\Delta\chi(E_i^*E_j-\tfrac{1}{3}|E(\omega,t)|^2\delta_{ij})+\text{c.c.} \quad (3)$$

Consider first the steady-state solution of Eq. (3). If the optical field propagating along $\hat{z}$ is linearly polarized, e.g., $\vec{E}=E\hat{x}$, we find immediately

$$Q_{xx}=-2Q_{yy}=\tfrac{1}{9}\Delta\chi|E(\omega)|^2/a(T-T^*). \quad (4)$$

The corresponding induced linear birefringence at ω' is

$$\delta n_l(\omega')=(2\pi/n)\tfrac{2}{3}\Delta\chi(\omega')(Q_{xx}-Q_{yy})=(2\pi/n)\Delta\chi(\omega)\Delta\chi(\omega')|E(\omega)|^2/9a(T-T^*), \quad (5)$$

where n is the linear refractive index. From the usual definition of the optical Kerr constant $B=\omega'\delta n_l/\pi c|E(\omega)|^2$, we have

$$B=2(\omega/nc)\Delta\chi(\omega)\Delta\chi(\omega')/9a(T-T^*). \quad (6)$$

If the intense optical field is elliptically polarized, e.g., $\vec{E}(\omega)=\hat{e}_+E_++\hat{e}_-E_-$ with $\hat{e}_\pm=(\hat{x}\pm i\hat{y})/\sqrt{2}$, we find from Eqs. (1) and (3) the following susceptibility tensor in the circular coordinates:

$$\frac{1}{2}\begin{pmatrix}\chi_{xx}+\chi_{yy}+i(\chi_{xy}-\chi_{yx}) & \chi_{xx}-\chi_{yy}-i(\chi_{xy}+\chi_{yx})\\ \chi_{xx}-\chi_{yy}+i(\chi_{xy}+\chi_{yx}) & \chi_{xx}+\chi_{yy}-i(\chi_{xy}-\chi_{yx})\end{pmatrix}=\bar{\chi}\delta_{ij}+\frac{(\Delta\chi)^2}{18a(T-T^*)}\begin{pmatrix}+\frac{1}{3}|E_+|^2+\frac{1}{3}|E_-|^2 & 2E_-^*E_+\\ 2E_-E_+^* & \frac{1}{3}|E_+|^2+\frac{1}{3}|E_-|^2\end{pmatrix}. \quad (7)$$

We can write for $\omega=\omega'$

$$\chi_{ij}(\omega)E_i^*(\omega)E_j(\omega)=\bar{\chi}|E(\omega)|^2+\delta\chi_+|E_+(\omega)|^2+\delta\chi_-|E(\omega)|^2,\qquad \delta\chi_\pm=[(\Delta\chi)^2/18a(T-T^*)][+\tfrac{1}{3}|E_\pm(\omega)|^2+\tfrac{7}{3}|E_\mp(\omega)|^2], \quad (8)$$

and then the field-induced refractive indices seen by the two circular components of the incoming elliptically polarized light are

$$\delta n_\pm(\omega)=(2\pi/n)\delta\chi_\pm(\omega). \quad (9)$$

The corresponding circular birefringence is

$$\delta n_c=\delta n_--\delta n_+=(2\pi/n)[(\Delta\chi)^2/9a(T-T^*)]\times[|\hat{e}_+^*\cdot\vec{E}(\omega)|^2-|\hat{e}_-^*\cdot\vec{E}(\omega)|^2]. \quad (10)$$

We shall see later that the above-mentioned induced linear and circular birefringences can be deduced from measurements of phase shifts of the linear and the elliptical polarizations, respectively. As seen in the above expressions, all these field-induced refractive indices and birefringences diverge as T approaches T^*. This critically divergent behavior is of course characteristic of a pretransitional phenomenon. In liquid-crystalline materials, the first-order transition temperature T_K ($>T^*$) always sets in before T reaches T^*.

In nonlinear optics, the field-induced refractive indices can be described more generally from symmetry considerations.[4,5] For an isotropic medium, the third-order nonlinear polarization takes the form

$$P_i^{(3)}(\omega') = \sum_j 6[\chi^{(3)}_{1122}(\omega' = \omega' + \omega - \omega)E_i(\omega')E_j(\omega)E_j^*(\omega) + \chi^{(3)}_{1212}(\omega' = \omega' + \omega - \omega)E_j(\omega')E_i(\omega)E_j^*(\omega) + \chi^{(3)}_{1221}(\omega' = \omega' + \omega - \omega)E_j(\omega')E_j(\omega)E_i^*(\omega)] , \quad (11)$$

where the $\chi^{(3)}$ are components of the third-order nonlinear susceptibility tensor. For $\omega = \omega'$, we have in circular coordinates

$$P_\pm^{(3)}(\omega) = 3(\chi^{(3)}_{1122} + \chi^{(3)}_{1212})|E_\pm(\omega)|^2 + (\chi^{(3)}_{1122} + \chi^{(3)}_{1212} + 2\chi^{(3)}_{1221})|E_\mp(\omega)|^2]E_\pm(\omega) . \quad (12)$$

We then find, for $\vec{E} = \hat{x}E$,

$$\delta n_{xx} = (2\pi/n)3(\chi^{(3)}_{1122} + \chi^{(3)}_{1212} + \chi^{(3)}_{1221})|E|^2 , \quad (13)$$

and, for $\vec{E} = \hat{e}_+E_+ + \hat{e}_-E_-$,

$$\delta n_\pm = (2\pi/n)3[(\chi^{(3)}_{1122} + \chi^{(3)}_{1212})|E_\pm(\omega)|^2 + (\chi^{(3)}_{1122} + \chi^{(3)}_{1212} + 2\chi^{(3)}_{1221})|E_\mp(\omega)|^2] , \quad (14)$$

$$\delta n_c = (2\pi/n)6\chi^{(3)}_{1221}[|\hat{e}_+^\dagger \cdot \vec{E}(\omega)|^2 - |\hat{e}_-^\dagger \cdot \vec{E}(\omega)|^2] .$$

Comparing Eqs. (13) and (14) with the previous expressions, we find, assuming $\Delta\chi(\omega) = \Delta\chi(\omega')$,

$$\chi^{(3)}_{1221} = 6\chi^{(3)}_{1122} = \tfrac{1}{6}(\Delta\chi)^2/9a(T - T^*) ,$$
$$\chi^{(3)}_{1212} = \chi^{(3)}_{1122} \quad (15)$$
$$B = 12(\omega/nc)\chi^{(3)}_{1221} .$$

Owyoung *et al.* have shown that with only a nuclear contribution the third-order nonlinear polarization can be written[6]

$$P_i^{(3)}(\omega) = \tfrac{1}{8}(2\alpha + \beta)E_i(\omega)E_j(\omega)E_j^*(\omega) + \tfrac{1}{4}\beta E_j(\omega)E_j(\omega)E_i^*(\omega) + \tfrac{1}{8}(2\alpha + \beta)E_j(\omega)E_i(\omega)E_j^*(\omega) . \quad (16)$$

In the case of liquid-crystalline materials, this is true since the electronic contribution is negligible compared to the nuclear part. We then have

$$\alpha = -24\chi^{(3)}_{1122} = -\tfrac{1}{3}\beta ,$$
$$\beta = 12\chi^{(3)}_{1221} , \quad B = (\omega/nc)\beta . \quad (17)$$

We now consider the transient case, where molecular ordering Q_{ij} is induced by an intense light pulse. From Eq. (3), we find immediately[1]

$$Q_{ij}(t) = \int_{-\infty}^{t} \frac{f_{ij}(t')}{\nu} e^{-(t-t')/\tau} , \quad (18)$$

where the orientational relaxation time is defined as

$$\tau = \nu/a(T - T^*) . \quad (19)$$

Consequently, we have

$$\delta n_i(t) = \frac{\pi c}{\omega} B\frac{1}{\tau}\int_{-\infty}^{t} |E|^2(t')e^{-(t-t')/\tau}dt' ,$$
$$\delta n_c(t) = \frac{\pi c}{\omega} B\frac{1}{\tau}\int_{-\infty}^{t} (|\hat{e}_+ \cdot \vec{E}|^2 - |\hat{e}_- \cdot \vec{E}|^2) \times (t')e^{-(t-t')/\tau}dt' . \quad (20)$$

Thus knowing the time variation of $\delta n_i(t)$ or $\delta n_c(t)$, we should be able to deduce the values of B and τ. Equation (19) shows that τ would diverge as T approaches T^*. This critical slowing-down behavior is again characteristic of a pretransitional phenomenon.

Suppose we have obtained B and τ as functions of temperature T. Then, from Eqs. (15) and (19), we can deduce the parameters T^*, $(\Delta\chi)^2/a$, and ν/a. If, in addition, $\Delta\chi$ is separately measured, then a and hence ν are also known. Now, the Landau–de Gennes model with the free-energy expression of Eq. (2) predicts[7] a first-order phase transition at $T_K = T^* + \frac{50}{243}b^2/ad$ and an order parameter $Q_K = \frac{20}{27}b/d$ at the transition. Knowing T_K, T^*, a, and Q_K, we can then deduce b and d,

$$b = \tfrac{18}{5}a(T_K - T^*)/Q_K , \quad d = 8a(T_K - T^*)T_K/Q_K^2 . \quad (21)$$

The validity of Eq. (21), however, depends on whether the Landau model gives a valid description of the isotropic-nematic transition.

III. EXPERIMENTAL ARRANGEMENT AND DATA ANALYSIS

A. Sample preparation

Our experimental work was on seven homologous compounds of *p,p'*-di-*n*-alkoxy-azoxybenzenes ($C_NH_{2N+1}O$-C_6H_4-N_2O-C_6H_4-OC_NH_{2N+1} with $N = 1, 2, \ldots, 7$). The samples were purchased from Eastman Kodak Company. Purification of the samples was done by recrystalization from a saturated solution in various solvents (see Table II). The recrystallized sample was then placed in an optical cell 2.5 cm long, which was evacuated for several hours to remove atmospheric H_2O and O_2 and the residual solvent. After evacuation, the sample

TABLE II. Solvents used for recrystallization of the *p,p'*-di-*n*-alkoxy-azoxybenzene homologous compounds.

N	Solvent
1	1-pentanol
2	1-pentanol
3	*n*-hexane
4	1-pentanol
5	acetone
6	acetone
7	acetone

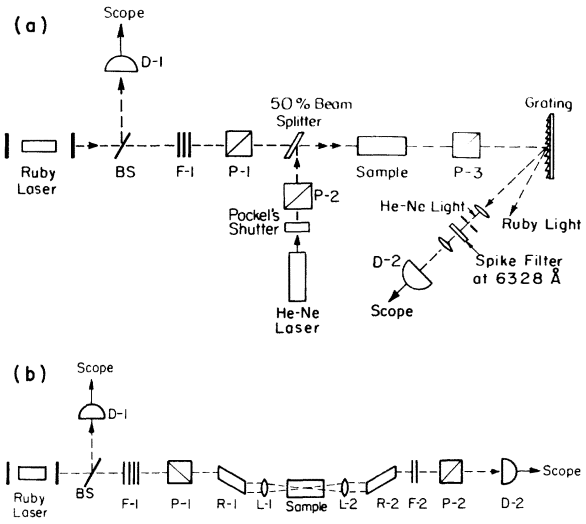

FIG. 1. (a) Experimental arrangement for observing molecular orientational relaxation times in nematic liquid crystals. BS, beam splitter; P-1, P-2, P-3, linear polarizers; D-1, ITT F4018 fast photodiode; D-2, RCA photomultiplier 7102; F-1, neutral-density stacks. (b) Experimental arrangement for observing ellipse-rotation effect. P-1, P-2, Glan polarizers; R-1, R-2, Fresnel rhombs; L-1, L-2, 15-cm lenses; F-1, F-2, neutral density stacks; D-1, D-2, ITT fast photodiodes.

cell was sealed under vacuum. A sample prepared this way was very homogeneous and had a sharp isotropic-nematic transition. The transition temperature was constant to within 0.1 °K for more than one month.

There was apparently a small amount of impurities in our samples, as evidenced by the lower transition temperatures than those reported for pure samples in the literature. The differences were typically less than 5 °K, suggesting an impurity concentration less than 1%. It appears that with such small impurity concentrations $T_K - T^*$ remains nearly unchanged. The temperature-dependent pretransitional properties as a function of $T - T^*$ should also remain unchanged and the material parameters deduced from our experiments should be insensitive to impurity contamination.[7]

During our optical measurements, the sample cell was placed in an oven with thermal control. The sample temperature was stablized to within 0.1 °K and its uniformity throughout the cell was better than 0.2 °K.

B. Experimental techniques

We obtained the orientational relaxation time τ from the measurements of transient optical Kerr effect, and the nonlinear refractive index or optical Kerr constant from the measurements of intensity-dependent ellipse rotation. The details of the experimental arrangements have already been described elsewhere.[1] Here, for the sake of clarity, we have reproduced the schematic diagrams of the experimental arrangements for the two types of measurements in Fig. 1.

In the optical Kerr measurements, the main difference between the present setup and the earlier one is that here we used a weakly mode-locked ruby laser instead of a Q-switched laser. This was necessary because τ for the homologous compounds can be as small as few nsec. The mode-locked pulses had a pulse width of about 1 nsec. A single pulse of ~20 kW switched out from the mode-locked train was used in the measurements to induce molecular ordering, and a 10-mW cw He-Ne laser was used to probe the ordering. In order to avoid any possible thermal lensing effect in the sample induced by the absorption of He-Ne laser light, a Pockell cell was employed to block the He-Ne laser beam until the arrival of the ruby laser pulse.

In the measurements of intensity-dependent ellipse rotation,[4] we used a single-mode Q-switched ruby laser. It had a pulse width of ~12 nsec and a peak power of ~100 kW. The beam was focused at the center of the sample cell. The length of the focal region was appreciably smaller than the cell length. With the output laser beam attenuated, the polarizer and the analyzer in Fig. 1(b) were set to be crossed with each other. The intensity-independent rotation of the elliptical polarization in the sample was then measured by the amount of light passing through the analyzer.

We also obtained the susceptibility anisotropy $\Delta\chi$ from the linear refractive-index measurements using the wedge method,[8] which is described in detail in Ref. 9. The refractive-index measurements at 6943 Å gave us χ_{xx} and χ_{yy} at $T \sim T_k - 20°$, while the magnetic resonance measurements[10] gave us the order parameter Q (~0.5) at the same temperature. Then, from Eq. (1), we could deduce $\Delta\chi$. We also measured the refractive indices n of the materials in the isotropic phase.

C. Data analysis

In our optical Kerr measurements, the signal detected was the He-Ne laser light transmitted through the sample between crossed polarizers. The signal S^{0K} was therefore proportional to $\sin^2(\omega' \delta n_l l/2c)$, where l is the sample length. The linear birefringence δn_l was induced by a laser pulse according to Eq. (20). In our case, $\delta n_l l \ll 1$, and hence we have

$$S^{0K}(t) \propto \left(B \int_{-\infty}^{t} |E(t')|^2 e^{-(t-t')/\tau} dt' \right)^2 , \qquad (22)$$

where $|E(t)|^2$ is the exciting laser pulse. The

above equation shows that if the laser pulse width is smaller than or comparable with τ, then at sufficiently large t the signal $S^{0K}(t)$ should decay exponentially as $e^{-2t/\tau}$. This was indeed the case in our measurements. From the exponential tail, we could deduce the relaxation time τ. In principle, since the exciting pulse $|E(t)|^2$ is known from the oscilloscope trace, we should be able to deduce not only τ but also the optical Kerr constant B from from the signal $S^{0K}(t)$. However, in the present case, the probing He-Ne laser beam was too weak to yield good signal-to-noise ratio for an accurate determination of B. We therefore used intensity-dependent ellipse rotation measurements instead to determine B.

For an infinite plane wave, the intensity-dependent ellipse rotation θ across the cell is given by[1,4,6]

$$\theta = (\omega/2c)\delta n_c l . \tag{23}$$

For a focused beam, however, θ is a function of radius r. Assume a single-mode laser pulse with a Gaussian profile focused at $z=0$:

$$|E|^2(r,z,t) = |\mathcal{E}_0|^2 \frac{W_0}{W^2(z)} \times \exp\left(-\frac{2r^2}{W^2(z)} - \alpha(z+\tfrac{1}{2}l) - \gamma^2 t^2\right), \tag{24}$$

where $W^2(z) = W_0^2[1+(2cz/\omega n W_0^2)^2]$, W_0 is the minimum radius of the focus, α is the power attenuation coefficient due to scattering and linear loss, and γ is a constant. The sample cell extends from $z=-\frac{1}{2}l$ to $z=\frac{1}{2}l$. Following the analysis of Owyoung[6] using the paraxial approximation, we can describe each cylindrically symmetric set of rays in the focused beam by a parameter K defined by

$$r^2 = K W^2(z) . \tag{25}$$

For each set of rays, the ellipse rotation is

$$\theta_K(t) = \int_{-l/2}^{l/2} (\omega/2c)\delta n_c(K,z,t)\,dz = \tfrac{1}{4}(|\mathcal{E}_0|^2 \cos 2\phi)(\pi^2 \omega n W_0^2/c) B L g(t) e^{-2K}, \tag{26}$$

where

$$L = \frac{2c}{\pi\omega n} e^{-\alpha l/2} \int_{-l/2}^{l/2} \frac{e^{-\alpha z}}{W^2(z)}\,dz ,$$

$$|\hat{e}_+ \cdot \vec{E}|^2 - |\hat{e}_- \cdot \vec{E}|^2 = |E|^2 \cos 2\phi , \tag{27}$$

$$g(t) = (\sqrt{\pi}/2\gamma\tau) e^{-1/4\gamma^2\tau^2}[1+\mathrm{erf}(\gamma t - 1/2\gamma\tau)] e^{-t/\tau} .$$

If the attenuation length $(1/\alpha)$ is much smaller than the longitudinal focal dimension $\omega n W_0^2/c$, then L can be approximated by

$$L = (2/\pi) e^{-\alpha l/2} [\tan^{-1}(c l/2\omega n W_0^2)] , \tag{28}$$

which reduces to $e^{-\alpha l/2}$ when $l \gg \omega n W_0^2/c$ and to 1 if, in addition, $l \ll 1/\alpha$.

We now have to integrate over all the rays in the beam to find the total power of the ellipically polarized light transmitted through the analyzer. In our case, $\theta_K \ll 1$, and hence the measured signal is

$$S^{ER}(t) = \int_0^\infty (\sin 2\phi)^2 \theta_K^2(t) P_K(t)\,dK , \tag{29}$$

where ER signifies ellipse rotation, and where

$$P_K(t)\,dK = (nc/4\pi)|E|^2(r, z=\tfrac{1}{2}l, t) 2\pi r\,dr = \tfrac{1}{4} n c W_0^2 |\mathcal{E}_0|^2 \exp(-2K - \alpha l - \gamma^2 t^2)\,dK .$$

We then have

$$S^{ER}(t) = (\pi^4 n^3 \omega^2 W_0^6/384c)|\mathcal{E}_0|^6 \sin^2 4\phi B^2 L^2 g^2(t) e^{-\alpha l - \gamma^2 t^2} . \tag{30}$$

Knowing $|\mathcal{E}_0|^2$ and ϕ, we can then determine the absolute value of the optical Kerr constant B.

In our experiment, we measured S_{max}^{ER} for the sample and used CS_2 as a reference whose Kerr constant is known. From Eq. (30), we find

$$\frac{B}{B_{CS_2}} = \left(\frac{S_{max}^{ER} e^{\alpha l}/L^2 \Gamma_{max} P_0^3}{S_{max}^{ER} e^{\alpha l}/L^2 \Gamma_{max} P_0^3)_{CS_2}} \right)^{1/2} , \tag{31}$$

where $\Gamma_{max} = [g^2(t) e^{-\gamma^2 t^2}]_{max}$ and P_0 is the incoming peak power. As seen from Eq. (30), S_{max}^{ER} is proportional to P_0^3. However, because of scattering and imperfect alignment, S_{max}^{ER} also has a residual term linear in P_0. Therefore we must measure

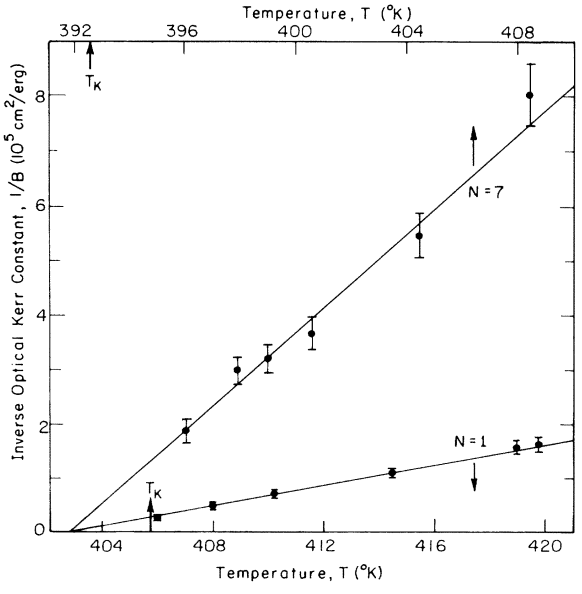

FIG. 2. Experimental results on optical Kerr constants vs temperature for $C_N H_{2N+1} O\text{-}C_6H_4\text{-}N_2O\text{-}C_6H_4\text{-}OC_n H_{2n+1}$, with $N=1$ and 7. The solid curves are calculated from Eq. (6).

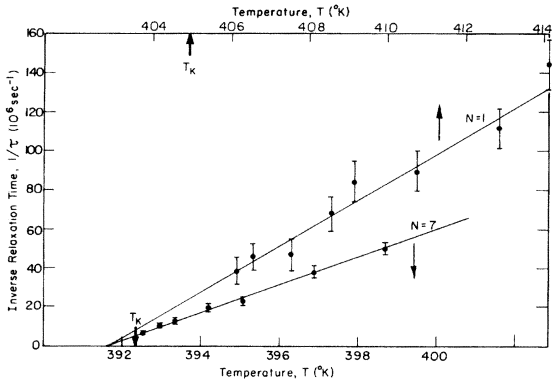

FIG. 3. Experimental results on orientational relaxation times vs temperature for $C_NH_{2N+1}O\text{-}C_6H_4\text{-}N_2O\text{-}C_6H_4\text{-}OC_NH_{2N+1}$, with $N=1$ and 7. The solid curves are calculated from Eq. (19).

S_{max}^{ER} as a function of P_0 and extract the term proportional to P_0^3 from the measurements.

We have measured τ, α, and B as functions of temperature in the isotropic phase for the seven homologous compounds of p,p'-di-n-alkoxy-azoxybenzenes. Using n and $\Delta\chi$ from our refractive-index measurements,[8] we then deduce the parameters ν, T^*, and a from Eqs. (6) and (19) for each compound.

IV. EXPERIMENTAL RESULTS

In Figs. 2 and 3, we show as examples the results of our measurements of τ and B, respectively, as functions of temperature for two p,p'-di-n-alkoxy-azoxzybenzene (PAA) compounds. Similar results were obtained for the other five compounds in the homologous series. In all cases, the data can be described very well by Eqs. (6) and (19). Strictly speaking, the viscosity coefficient ν in Eq. (6) is not temperature independent. One often expresses $\nu(T)$ in the form

$$\nu(T) = \nu_0 e^{-WT}, \tag{32}$$

where W is a constant. However, in our cases, because the investigation was limited to a narrow temperature range, we can approximate $\nu(T)$ by $\nu(T_K)$. The error introduced by this approximation is less than 4%. Thus by fitting the experimental data with the theoretical curves of Eqs. (6) and (19), we can deduce T^*, ν/a, and $(\Delta\chi)^2/a$ for each compound. From the independently measured values of $\Delta\chi$,[8] we then obtain ν and a separately. As discussed in Sec. II, if we believe in the Landau's expansion at the isotropic-nematic transition, we can also deduce the parameters b and d for these compounds using Eq. (21). Here, T_K's were measured, and the Q_K's were obtained from

$$Q_K = [\chi_{xx}(T_K) - \chi_{yy}(T_K)]/\Delta\chi$$

by extrapolating our linear refractive-index measurements to T_K.[8] These Q_K differed by ~10% from those measured directly by magnetic resonance at $T = T_K$,[10] partly owing to larger uncertainty in the magnetic-resonance measurements at T_K, and partly because of inaccuracy in our extrapolation.

We have listed in Table III the values of $(T - T^*)\tau$, $(T - T^*)B$, and other parameters deduced from our measurements for the seven compounds of the homologous series. We have then plotted, as functions of the number of carbon atoms in the alkyl chain at either end of the molecule, $(T - T^*)\tau$ and $(T - T^*)B$ in Fig. 4, T^*, T_K, and ΔH in Fig. 5, ν and $\Delta\chi$ in Fig. 6, and a, b, and d in Fig. 7.

In our relaxation measurements, shot noise in the photomultiplier was the main source of experimental uncertainty. Typical error of about ± 10% is represented by the error bars in Fig. 2, where each data point was the result of averaging over more than four laser shots. This uncertainty can of course be improved by using a probe beam of stronger intensity. As the relaxation time τ approaches the response time of the detection system (≲7 nsec in our case), the uncertainty would of course become larger unless the signal is properly deconvoluted.

The ellipse-rotation measurements had an accur-

TABLE III. Various characteristic parameters of the p,p'-di-n-alkoxy-azoxybenzene homologs deduced from the experiment.

N	$T_K - T^*$ (°K)	$\tau\Delta T$ (10^{-9} sec °K)	$B\Delta T$ (10^{-5} esu)	ν (10^{-3} P)	a (10^5 erg/cm^3 °K)	b (10^7 erg/cm^3)	d (10^7 erg/cm^3)	ΔH_{th} (10^6 erg/cm^3)
1	3.0	90	10.5	62.6	6.69	21.0	41.1	33.9
2	3.8	80	9.2	52.1	6.52	19.4	27.3	56.9
3	2.75	180	9.0	95.9	5.33	15.0	29.7	24.6
4	4.9	155	8.9	68.9	4.45	17.9	29.1	30.3
5	4.4	240	6.4	135.4	5.57	24.1	49.4	20.9
6	0.9	150	3.9	105.1	7.00	4.4	6.9	39.8
7	0.7	140	2.2	151.3	10.81	6.0	10.1	59.0

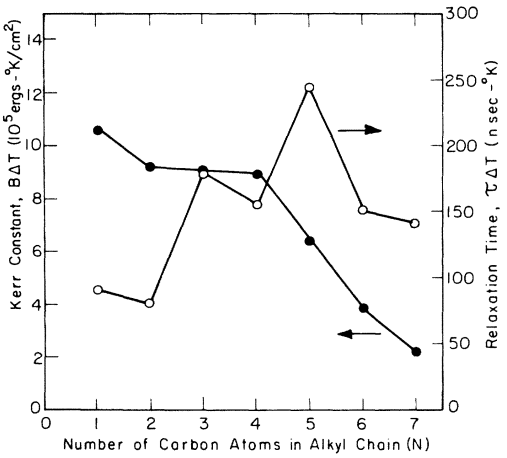

FIG. 4. Experimental values of $(T-T^*)B$ and $(T-T^*)\tau$ for the first seven p,p'-di-n-alkoxy-azoxybenzene homologs.

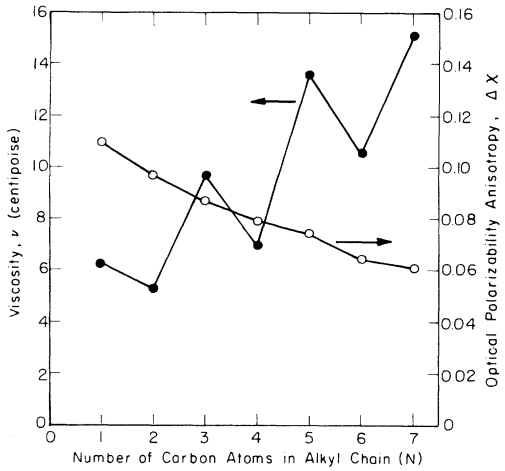

FIG. 6. Values of ν and $\Delta\chi$ for the first seven p,p'-di-n-alkoxy-azoxybenzene homologs.

acy better than 2% so far as the signal S^{ER}_{max}/P_0^3 was concerned. However, in deducing the optical Kerr constant from Eq. (31), the uncertainty in the relaxation time τ came in through $g(t)$. Together with the uncertainty ($\sim\pm 5\%$) in determining L, this led to an overall uncertainty of $\sim\pm 15\%$ in the values of B shown in Fig. 2.

V. DISCUSSION

Figures 4–7 show how the increase of alkyl-chain length by the addition of methylene groups modifies the physical behavior of the homologous compounds. Here, we give a brief qualitative discussion of the results.

Figure 4 shows that the seven homologous compounds all have a large Kerr constant and a long relaxation time, which are characteristics of other liquid-crystalline materials.[1] For the same $\Delta T = T - T^*$, $B\Delta T$ drops appreciably as N increases, mainly owing to a drop in $\Delta\chi$, shown in Fig. 6. On the other hand, $\tau\Delta T$ has a zigzag behavior with increase of N. It is the result of the zigzag behavior of ν also shown in Fig. 6.

In Fig. 5, we notice that a regular alteration of the isotropic-nematic transition temperatures T_K and T^* and the latent heat ΔH occurs between homologs containing odd and even numbers of carbon atoms in the alkyl chain. For T_K and ΔH, this is a common behavior for many homologous series of liquid-crystalline compounds and is known to be the result of the cog-wheel arrangement of the carbon atoms along the alkyl chain. That the fictitious second-order transition temperature T^* also has such a behavior is a manifestation of the weak first-order transition characteristics of these compounds. Because of that, T_K and T^* never differ by more than 5 °K. We

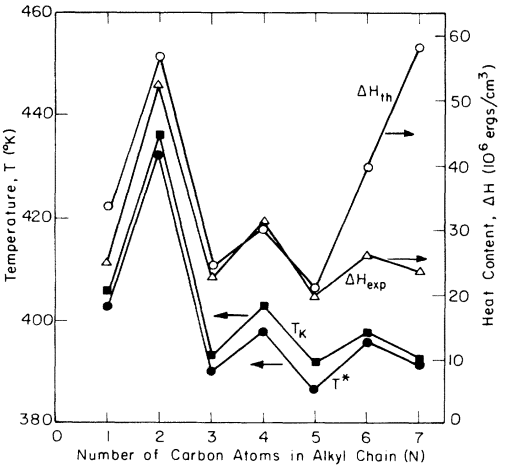

FIG. 5. Experimental values of T_K, T^*, and ΔH_{expt} for the first seven p,p'-di-n-alkoxy-azoxybenzene homologs. The values of ΔH_{th} were deduced from Eq. (34) using experimental values of a, T_K, and Q_K.

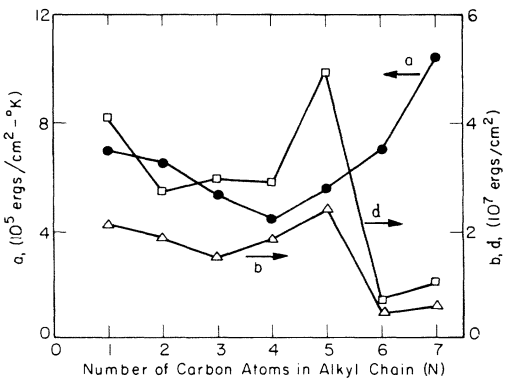

FIG. 7. Values of the Landau expansion coefficients a, b, and d [see Eq. (2)] deduced from experiment for the first seven p,p'di-n-alkoxy-azoxybenzene homologs.

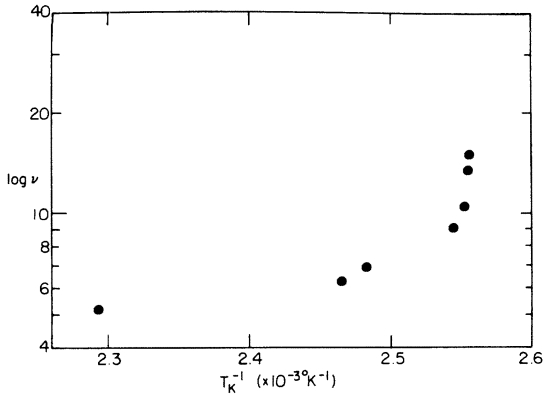

FIG. 8. Plot of $\log\nu$ vs T_K^{-1} showing that the experimental data do not fall on a straight line.

also notice in Fig. 5 that $T_K - T^*$ becomes appreciably smaller for $n=6$ and 7. This seems to suggest that the longer chains on the molecules make the transition closer to second order, presumably because of the stronger waggling motion of the end segment and the falling off of the terminal interaction.

The viscosity coefficient ν shown in Fig. 6 also alters regularly between homologs containing odd and even numbers of carbon atoms in the alkyl chain. This is caused by the strong temperature dependence of ν, as suggested in Eq. (32). In the present case, we can approximate $\nu(T)$ by $\nu(T_K)$. Then, according to Eq. (32), we expect to find smaller ν for compounds with large T_K and hence the qualitative behavior of ν in Fig. 6. However, we should not expect the constants ν_0 and W in Eq. (32) to be the same for all the compounds in the homologous series. If they were, we would find $\log\nu(T_K)$ vs T_K^{-1} to be a straight line from which we could deduce ν_0 and W. As shown in Fig. 8, this is certainly not the case for the PAA homologs.

The optical anistropy $\Delta\chi$ in Fig. 6 shows a fairly smooth decrease with increase of the chain length. In fact, on the microscopic scale, the molecular polarizability anisotropy $\Delta\alpha$ actually increases with the increase of chain length, as one would intuitively expect.[8] $\Delta\chi$ behaves differently from $\Delta\alpha$ because of the molar volume effect. The medium with longer chain molecules has a lower molecular density. Its effect on $\Delta\chi$ turns out to be larger than the incremental effect of $\Delta\alpha$ on $\Delta\chi$, owing to the addition of methylene groups on the chain.

Figure 7 shows that the variations of the Landau parameters a, b, and d with chain length do not have any regular pattern. The physical meanings of a, b, and d often depend on the model describing the intermolecular interaction. In the mean-field theory of Maier and Saupe,[11] we should expect a to be a constant independent of the compounds. The values of a for the seven homologous compounds in Fig. 7, however, vary over a factor of 2. This suggests that the mean-field theory for isotropic-nematic transition is actually a poor approximation. The values of b and d in Fig. 7 were deduced by assuming the Landau expansion of free energy is valid at the isotropic-nematic transition. To check the validity of the Landau expansion, we insert the values of a, b, and d in Eq. (2) with $Q \sim 0.4$ and $T = T_K$. We find that the b and d terms in Eq. (2) are often larger than the a term, indicating a divergence or poor convergence of the power-series expansion. Thus at least the truncated Landau expansion in the form of Eq. (2) is not valid at $T = T_K$. The values of b and d given in Fig. 7 are therefore not very meaningful. For $T > T_K$ and $Q < 0.01$, however, Eq. (2) is valid. With the values of b and d given in Fig. 7, and for $Q < 0.01$, the b and d terms in Eq. (2) become negligible. This was true in our experiment, where Q was always less than 10^{-3}.

In the literature, the Landau expansion has also been used to derive the heat content ΔH of a first-order transition,

$$\Delta H = \frac{3aT_K Q_K^2}{4} + \frac{5}{12}\left(\frac{\partial b}{\partial T}\right)_{T_K} Q_K^3 + \frac{9}{32}\left(\frac{\partial d}{\partial T}\right)_{T_K} Q_K^4 . \tag{33}$$

If we neglect the $\partial b/\partial T$ and $\partial d/\partial T$ terms, we then have

$$\Delta H = \tfrac{3}{4} aT_K Q_K^2 . \tag{34}$$

The above equation was used by Stinson *et al.*[7] Using the values of a, T_K, and Q_K listed in Tables I and III for the homologous compounds, we find the values of ΔH shown in Fig. 5 as $\Delta H_{\rm th}$. Compared with the directly measured values $\Delta H_{\rm expt}$, the agreement is fairly good for all compounds except $N=6$ and 7. The discrepancy could be due to neglect of b and d terms in Eq. (33) or due to failure of the Landau expansion. It may also be the result of residual short-range smectic order at T_K, since the $N=6$ and $N=7$ homologs are known to have a smectic phase at lower temperatures. The rapid rise of $\Delta H_{\rm th}$ towards $N=6$ and 7 comes from the corresponding sharp rise of a, which in turn is the result of the quick drop of $B(T - T^*)$ towards $N=6$ and 7.

VI. CONCLUSION

Using ellipse rotation and the transient optical Kerr effect, we have measured the third-order nonlinear susceptibility (or the optical Kerr constant B) and the corresponding relaxation time τ

for seven nematic compounds of the p,p'-di-n-alkoxy-azoxybenzene homologous series as functions of temperature in the isotropic phase. The results showing critical divergence of B and critical slowing down of τ are in good agreement with predictions from the Landau–de Gennes model. Similar in characteristics to other liquid-crystalline materials, all these compounds have a large Kerr constant and a long relaxation time strongly dependent on temperature. Together with the existing data on optical anisotropy and the order parameter at the nematic-isotropic transition, we have deduced various characteristic parameters of the nematic compounds. These include the fictitious second-order transition temperature T^*, the orientational viscosity ν, the Landau expansion coefficients a, b, and d, the heat content ΔH, etc. The results show how these characteristic parameters vary among the homologous series as the alkyl-chain length of the molecules increases through addition of methylene groups to the chain. Part of the results can be understood from the molecular structural point of view. The variation of the Landau parameter a with compounds indicates that the mean-field theory of Maier-Saupe is not a good approximation to describe the isotropic-nematic transition. Our values of a, b, and d also suggest that the Landau-series expansion of the free energy is a poor approximation at the transition. The heat contents ΔH derived from the expression $\Delta H = \frac{3}{4} a T_K Q_K^2$ deviates appreciably from the experimental values for the higher members of the homologous series.

ACKNOWLEDGMENTS

We want to thank Professor A. Pines and Dr. D. J. Ruben for letting us use their NMR results on order parameters prior to publication. We are grateful to the Material and Molecular Research Division of the Lawrence Berkeley Laboratory for providing us with some of the experimental facilities. One of us (Y.R.S.) wishes to acknowledge the support of a research professorship at The Miller Institute of the University of California.

---

*Supported by National Science Foundation Grant No. DMR74-07361.

†On leave at The Miller Institute of Univ. of California.

[1]G. K. L. Wong and Y. R. Shen, Phys. Rev. Lett. 30, 895 (1973); Phys. Rev. A 10, 1277 (1974); J. Prost and J. R. Lalanne, *ibid.* 8, 2090 (1973).

[2]H. Arnold, Z. Phys. Chem. (Leipz.) 226, 146 (1964).

[3]P. G. de Gennes, Phys. Lett. 30A, 454 (1969); Mol. Cryst. Liq. Cryst. 12, 193 (1971).

[4]P. D. Maker and R. W. Terhune, Phys. Rev. 137, A801 (1965).

[5]P. N. Butcher, *Nonlinear Optical Phenomena*, (University Engineering, Columbus, 1965).

[6]A. Owyoung, R. W. Hellwarth, and N. George, Phys. Rev. A 4, 2342 (1971); 5, 628 (1972); A. Owyoung, IEEE J. Quantum Electron. QE-9, 1064 (1973).

[7]T. W. Stinson and J. D. Litster, Phys. Rev. Lett. 25, 503 (1970); T. W. Stinson, J. D. Litster, and N. A. Clark, J. Phys. (Paris) 33, 69 (1972).

[8]E. G. Hanson and Y. R. Shen (unpublished).

[9]I. Haller, H. A. Huggins, and M. J. Freiser, Mol. Cryst. Liq. Cryst. 16, 53 (1972); I. Haller, H. A. Huggins, H. R. Lilienthal, and T. R. McGuire, J. Chem. Phys. 77, 950 (1973).

[10]A. Pines, D. J. Ruben, and S. Allison, Phys. Rev. Lett. 33, 1002 (1974); more refined data are given by A. J. Pines and D. J. Ruben (unpublished).

[11]W. Maier and A. Saupe, Z. Naturforsch. A 13, 564 (1958); 14, 882 (1959); 15, 287 (1960).